Article

Development of a New Generalizable, Multivariate, and Physical-Body-Response-Based Extreme Heatwave Index

Marcio Cataldi [1,2,3,*], Vitor Luiz Victalino Galves [2], Leandro Alcoforado Sphaier [4], Ginés Garnés-Morales [1], Victoria Gallardo [1], Laurel Molina Párraga [1], Juan Pedro Montávez [1] and Pedro Jimenez-Guerrero [1]

[1] Regional Atmospheric Modelling Group (MAR), Physics of the Earth, Department of Physics, Regional Campus of International Excellence (CEIR) "Campus Mare Nostrum", University of Murcia, 30100 Murcia, Spain; gines.g.m@um.es (G.G.-M.); laurel.molinap@um.es (L.M.P.); montavez@um.es (J.P.M.); pedro.jimenezguerrero@um.es (P.J.-G.)

[2] Climate System Monitoring and Modeling Laboratory, Water Resources and Environmental Engineering, Federal Fluminense University, Niterói 24220-900, Brazil; vitor_luiz@id.uff.br

[3] Natural Hazards and Risk Analysis (NHaRA) Group, Barcelona Supercomputing Centre, 08034 Barcelona, Spain

[4] Laboratory of Thermal Sciences—LATERMO, Department of Mechanical Engineering, Federal Fluminense University—PGMEC/UFF, Rua Passo da Pátria 156, Bloco D, Sala 302, Niterói 24210-240, Brazil; lasphaier@id.uff.br

* Correspondence: mcataldi@id.uff.br

Abstract: The primary goal of this study is to introduce the initial phase of developing an impact-based forecasting system for extreme heatwaves, utilizing a novel multivariate index which, at this early stage, already employs a combination of a statistical approach and physical principles related to human body water loss. This system also incorporates a mitigation plan with hydration-focused measures. Since 1990, heatwaves have become increasingly frequent and intense across many regions worldwide, particularly in Europe and Asia. The main health impacts of heatwaves include organ strain and damage, exacerbation of cardiovascular and kidney diseases, and adverse reproductive effects. These consequences are most pronounced in individuals aged 65 and older. Many national meteorological services have established metrics to assess the frequency and severity of heatwaves within their borders. These metrics typically rely on specific threshold values or ranges of near-surface (2 m) air temperature, often derived from historical extreme temperature records. However, to our knowledge, only a few of these metrics consider the persistence of heatwave events, and even fewer account for relative humidity. In response, this study aims to develop a globally applicable normalized index that can be used across various temporal scales and regions. This index incorporates the potential health risks associated with relative humidity, accounts for the duration of extreme heatwave events, and is exponentially sensitive to exposure to extreme heat conditions above critical thresholds of temperature. This novel index could be more suitable/adapted to guide national meteorological services when emitting warnings during extreme heatwave events about the health risks on the population. The index was computed under two scenarios: first, in forecasting heatwave episodes over a specific temporal horizon using the WRF model; second, in evaluating the relationship between the index, mortality data, and maximum temperature anomalies during the 2003 summer heatwave in Spain. Moreover, the study assessed the annual trend of increasing extreme heatwaves in Spain using ERA5 data on a climatic scale. The results show that this index has considerable potential as a decision-support and health risk assessment tool. It demonstrates greater sensitivity to extreme risk episodes compared to linear evaluations of extreme temperatures. Furthermore, its formulation aligns with the physical mechanisms of water loss in the human body, while also factoring in the effects of relative humidity.

Keywords: climate change; climate and health; extreme events; prevention and mitigation; atmospheric modeling

1. Introduction

Heatwaves (HWs) have become increasingly prolonged and intense in many regions worldwide, especially across Europe and Asia since the 1990s, though their impact is not limited to these areas [1]. As documented by [2], the primary health impacts of HWs on populations include heat-related illnesses and deaths, as well as increased rates of cardiovascular and kidney diseases and adverse reproductive outcomes. These harmful effects are observed globally, with individuals over 65 years old typically being the most affected [3–8].

The high mortality rates linked with HW episodes potentially stem from a variety of factors, including inadequately prepared housing for high-temperature conditions (typically constructed for cold isolation), lack of cooling infrastructure in housing, pre-existing kidney, lung, and/or cardiovascular illnesses, social isolation, low social status, and the lack of habit of consuming an adequate amount of water on a daily basis, especially for the elderly [9–11]. Additional factors, such as urban heat islands, air quality, and potential power outages during HWs, are also significant contributors to mortality rates [12–15].

When examining factors related to mortality rates during HWs, it becomes clear that this is an emerging phenomenon, predominantly impacting countries more accustomed to cooler climates than to high temperatures [16–18]. Regarding the impact of HWs in developing nations, it is important to consider the precarious public health conditions and lack of basic sanitation, which are prevalent in a significant portion of these countries. These factors should be regarded as additional risk factors, in addition to those previously outlined [19,20].

Given that HW incidents tend to intensify and occur more frequently, as evidenced in [21] and, more recently, in [22], it is imperative to construct and implement public policies that provide greater resilience to individuals and nations in the face of this sort of occurrence. Between 1981 and 2023, it is estimated that around 250,000 deaths may have been linked to temperature extremes, with approximately 87% of these happening in Europe. The study in [17] and the database contained in [23] were used to support these values.

Many countries have implemented indices to assess the frequency of HW episodes within their borders. These indices typically rely on thresholds or air temperature ranges measured at 2 m above ground, reflecting extreme percentiles derived from historical records. While some of these indices also consider the persistence of HW events and assess the health risks of elevated temperatures in a linear fashion, they often lack a comprehensive statistical approach that integrates physical phenomena, such as water loss in the human body. The review conducted in the study of [24] highlights this gap, underscoring the need for indices that better capture the physiological impacts of HWs.

When the relationship between rising temperatures, after exceeding a certain threshold, and health risks is considered linear, these risks may be significantly underestimated within the population. This may result in a skewed perception of the actual risk involved. Moreover, some studies highlight the significant role of relative humidity in the loss of body water during HW episodes, also emphasizing the link between this abrupt water loss and the occurrence of thrombosis and heart attacks, which elevates the possibility of enduring potentially fatal diseases [25–28].

The reality is that the role of relative humidity in increasing mortality rates associated with heat waves is still not very clear or well understood and has even been contested in some studies that rely purely on statistical models, particularly in metropolitan regions like Paris, as discussed in the article by [29]. It is worth noting that, in this study, the authors concluded that relative humidity had little influence, despite analyzing data from only 2 meteorological stations with humidity records, compared to 25 stations that provided air temperature data. Nonetheless, this study presents an approach that illustrates, both physically and mathematically, the influence of relative humidity, as well as the nonlinear behavior of temperature's impact on human body water loss rates.

HW episodes that are intense and persistent enough to directly impact human health will be referred to in this study as extreme heatwave episodes (XHWIs), drawing on previous studies that have similarly classified intense and prolonged episodes [30,31].

To comprehensively assess the health risks linked with XHW events, it is crucial to acknowledge the significant variability in climate worldwide, alongside the diverse reactions of living organisms to extreme temperature and humidity conditions. Additionally, each individual's gender, ethnicity, age, pre-existing medical conditions, and geographical location should be considered [1].

This paper aims to initiate the development of an XHWI that could have global applicability, since this index can be calibrated using mortality rate data associated with HWs, or it can be applied in regions lacking such data, as its mathematical formulation already integrates the key physical mechanisms that link XHW events to health risks. To achieve this, it takes into consideration the statistical distributions of temperature and relative humidity in the region of study, while also accounting for the duration of the XHW and the exponential relationship with higher temperatures, to reduce health risks.

The proposed XHWI values must increase exponentially with rising temperatures, as water loss from the body due to perspiration also escalates exponentially beyond a certain temperature threshold. This will be demonstrated both physically and mathematically in the following section. It implies that, beyond specific temperature limits, the associated risk should increase exponentially rather than linearly with rising air temperature.

The developed index was applied to quantify three selected XHW episodes as case studies: (i) a comparison of the index's behavior with maximum temperature anomalies and mortality series during the 2003 XHW in Spain; (ii) a forecast of an isolated XHW episode in Rio de Janeiro, Brazil, that occurred in 2023; and (iii) an analysis of the annual progression of XHW episodes during the summer from 1950 to 2022 across five cities in Spain.

The heterogeneity of the case studies chosen for this work is due to the intention of assessing the behavior of the index and its mathematical derivatives across different spatial and temporal scales, as well as under both diagnostic and prognostic conditions.

2. Theoretical Background—Relationship Between Body Water Loss and Temperature

As temperature rises, the body's need to regulate its internal temperature becomes more critical. The primary mechanism for this is sweating, where the evaporation of sweat from the skin surface promotes body cooling. While this process is essential for controlling body temperature, it can lead to a significant loss of body water, which research shows increases exponentially with temperature, highlighting the critical nature of temperature thresholds [32]. Experimental data [33] show that the volumetric sweat rate (in liters/min) may be expressed as (considering a person at rest):

$$\dot{V}_{sweat} = 0.55(T_c - 36.5) - 0.455(T_c - 36.35)(1 - \exp[-2.7(33 - T_s)]) \tag{1}$$

where T_c represents the body core temperature and T_s is the skin temperature, valid for body temperatures above 36.5 °C. This expression shows that the sweat rate increases exponentially with skin temperature once it exceeds 32 °C, as can be seen in Figure 1.

The following Equations (2)–(6) and their analyses can be found in [34]. In a warm environment, to maintain the body core temperature T_c, the body must reject the generated heat $\dot{Q}_c$, which is accomplished via skin heat loss $\dot{Q}_s$ and respiration heat loss $\dot{Q}_r$:

$$\dot{Q}_c = \dot{Q}_s + \dot{Q}_r \tag{2}$$

The skin heat loss can be written in terms of a body thermal resistance R_b connecting the core and skin temperatures:

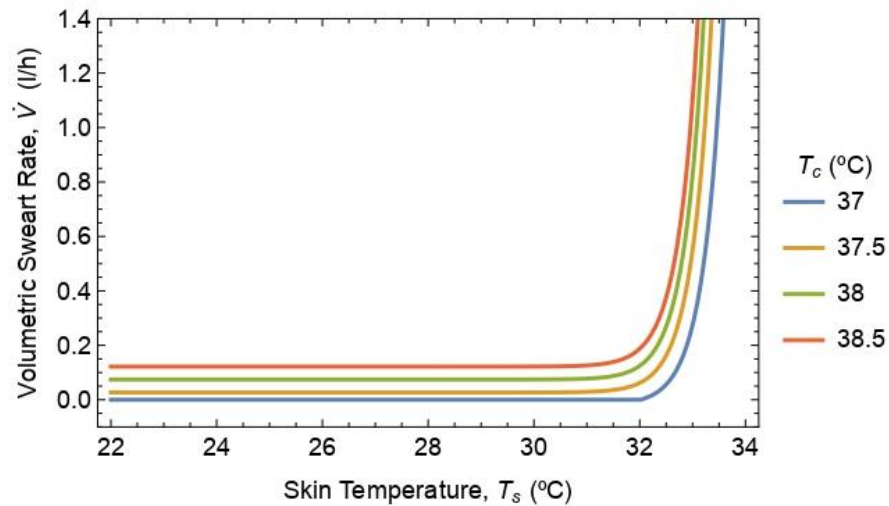$$\dot{Q}_s = \frac{T_c - T_s}{R_b} \tag{3}$$

Figure 1. Empirical relationship between the volumetric sweat rate, skin temperature, and ambient temperature, as per Equation (1).

This resistance will vary within certain limits to regulate body temperature; for a warm environment, it will decrease to lower values, as this condition leads to higher skin temperatures. Although R_b can vary, it cannot be lowered below a minimum value, meaning that, in extreme heat, if the skin temperature cannot be lowered, the body core temperature will increase, thus leading to hyperthermia.

The skin temperature will depend on the heat transfer between the skin and environment, which can be written in terms of sensible components (due to convection and radiation) and a latent component (due to sweat evaporation):

$$\dot{Q}_s = \dot{Q}_{conv} + \dot{Q}_{rad} + \dot{Q}_{evap} \tag{4}$$

where

$$\dot{Q}_{conv} = h_h A_s (T_s - T_{en}) \tag{5}$$

$$\dot{Q}_{rad} = A_s \sigma \left(\epsilon_s T_s^4 - \epsilon_{en} T_{en}^4 \right) \tag{6}$$

in which h_h is the convective heat transfer coefficient, A_s is the body surface area, ϵ_s is the skin emissivity and ϵ_{en} is the environmental emissivity (assuming gray and diffuse surfaces), σ is the Stephan Boltzmann constant ($5.67 * 10^{-8}$ W/m^2 * K^4), and T_{en} is the environment temperature, which is treated as a blackbody. The case without direct solar irradiation on the skin is considered.

The rate of evaporation can be expressed as [35]

$$\dot{m}_{evap} = h_m \rho_a (Y_s - Y_{en}) \tag{7}$$

and the heat transfer due to evaporation can be directly calculated from $\dot{Q}_{evap} = i_{lv} \dot{m}_{evap}$, where i_{lv} is the latent heat of water evaporation, h_m is the convective mass transfer coefficient, ρ_a is the density of dry air, and Y_s and Y_{en} are humidity ratios for the air on the skin surface and the environment. These can be written in terms of the relative humidity ϕ as [36]

$$Y = r_M \frac{\phi P_{sat}}{P - \phi P_{sat}} \tag{8}$$

where P is the atmospheric pressure, r_M is the molecular masse ratio of water to dry air, and P_{sat} is the vapor saturation pressure, which depends on temperature.

For environment temperatures near the body temperature T_c, the skin heat transfer rate is primarily driven by evaporation. In these conditions, if the environmental relative

humidity is high, evaporation will be significantly reduced (reaching zero for $\phi_{en} = 100\%$), raising the skin temperature and exponentially increasing the sweat rate. It's important to note that the rate of sweat production and sweat evaporation are not equal. A person continues to sweat in warm environments, but if the relative humidity is high, the sweat will not evaporate effectively. In extreme heat, where environmental temperatures exceed normal body temperature, as can occur during XHWs, the situation worsens. Heat transfer through convection and radiation may heat the skin instead of cooling it, and evaporation may cease even before relative humidity reaches 100%. In these cases, skin temperature rises even more rapidly, causing an exponential increase in water loss through sweating.

Thus, beyond certain environmental temperature and relative humidity thresholds, the risk associated with water loss increases exponentially, not linearly. Therefore, when designing indices or assessing risks related to temperature increases, it is crucial to reflect this exponential relationship. Indices that assume a linear relationship may underestimate the risk and fail to capture critical points where dehydration and heat-related illnesses spike dramatically [37]. The exponential nature must be considered in models and assessments to ensure an accurate representation of the potential risks involved with rising temperatures [38,39].

3. Methodology

This methodology section is divided into four subsections: the first describes the mathematical calculation of the index; the second details its application in the XHW episode that occurred in Spain in 2003; the third details its application in the XHW episode that occurred in March 2024 in the city of Rio de Janeiro through a simulation using the WRF model; and the fourth discusses the application of the index on a climate scale, addressing the trend of XHW evolution in five cities in Spain.

3.1. Index Calculation

3.1.1. Obtaining the Probability Distribution Function (PDF) of Maximum Temperatures

The first phase for calculating the index is obtaining the probability distribution function (PDF) of the maximum temperatures for the location where it will be applied, which should preferably be performed during a period with no trend in maximum temperature variation or with the smallest possible trend. At least 30 years of data should be used for this step. In this phase, only daily maximum temperature data will be required, in order to obtain the PDF of the maximum temperature, along with the temperature value equivalent to the 95th percentile of this distribution.

For this study, ECMWF Reanalysis version 5 [40] data were used for the grid points closest to the cities of Rio de Janeiro, Brazil, and Murcia, Madrid, Teruel, Caceres, and Córdoba, Spain, during the period from 1960 to 1990. This distribution can be obtained for the temperatures of a specific month or for a two-month or even a three-month period, depending on the seasonality of the region.

3.1.2. Mathematical Formulation of the Index

Based on the discussion in Section 2 (Equation (1)), it is understood that an index capable of efficiently assessing the health risks associated with XHWs, particularly in relation to dehydration and its consequences, should take into account relative humidity and consider the exponential increase in risk as temperatures rise, especially when ambient temperatures exceed 32 °C (assuming heat exchange without loss through the skin). This threshold can be calibrated for different situations and physiological profiles.

In this sense, the index should be a function of both temperature and humidity, as specified in Equation (9):

$$I = f(T) * g(\phi) \tag{9}$$

In this case, $f(T)$ should be a function that considers the exponential increase in temperature. The proposed form for $f(T)$ is the following (Equation (10)):

$$f(T) = e^{T_{pe}} \tag{10}$$

in which T_{pe} is the cumulative probability of extreme temperatures, representing how much the maximum recorded or predicted temperature for a given hour exceeds 95% of the PDF of average maximum temperatures for that month (or seasonal period). This is a dimensionless value, as it refers to the value of the distribution. For example, if the predicted or observed maximum temperature for a given hour falls within 97.4% of the distribution, the value of T_{pe} will be 2.4.

The function related to relative humidity, $g(\phi)$, should be proportional to the relative humidity to preserve the dimensionless nature of the index. However, it must be adjusted by a factor to balance its influence with $f(T)$. This adjustment was made empirically, since there are still no studies that physically describe how this relationship might behave in a more generalized situation, leading to Equation (11):

$$g(\phi) = \frac{\phi}{1000} \tag{11}$$

The quantity ϕ is the predicted or observed relative humidity for that hour. The relative humidity must be considered with its actual value, regardless of the humidity distribution for a given region, as it will be considered physically in relation to the loss of water, together with the temperature value.

It is important to emphasize that the index grows exponentially when temperatures exceed the 95th percentile of the distribution, significantly amplifying the risk associated with HW due to its reliance on extreme temperature values.

Finally, the semi-empirical index proposed in this study will produce non-zero values only when the air temperature at a given hour exceeds 32 °C and simultaneously surpasses the 95th percentile of the cumulative distribution of maximum temperatures obtained during calibration. This is outlined in Equation (12), and from this point forward, it will be referred to as the XHWI.

$$XHWI = e^{T_{pe}} * \frac{\phi}{1000} \tag{12}$$

For this index to be applicable and serve as a reliable basis for comparison anywhere in the world, it is essential that it be normalized. Once normalized, with values ranging from 0 to 1, it can be further adjusted for each city or region based on mortality rates associated with XHWI episodes. This allows different risk levels to be assigned to each tier of the index.

Accordingly, Equation (13) presents a proposed normalization for the index ($XHWI_N$), assuming the minimum relative humidity (ϕ_{min}) is 1%. This value was chosen to ensure that the index can be applied anywhere in the world. While the minimum relative humidity during an XHW episode typically ranges between 10% and 12% [41], relative humidity values slightly below 1% have been observed in places like Nevada, USA, and Iran [42]. This justifies the selection of this value.

$$XHWI_N = \frac{XHWI - \frac{\phi_{min}}{1000}}{XWMI_{max} - \frac{\phi_{min}}{1000}} \tag{13}$$

where (considering the maximum T_{pe} value of 5 and a relative humidity of 100%)

$$XWMI_{max} = \frac{e^5}{10} \tag{14}$$

The index $XHWI_N$ should be calculated for each hour of the day, and, for risk assessment purposes, it is recommended that the sum of the index value for a given day be multiplied by the number of hours the index was greater than zero (Equation (13)), creating a product that reflects not only the intensity of the HW but also its persistence.

$$XHWI_{Nday} = XHWI_{Nsum} * H_{NZ} \tag{15}$$

where $XHWI_{N\,day}$ is the value of the daily $XHWI_N$ index product, which can be used both to create a risk indicator for a specific day, based on numerical weather model forecasts, and to be accumulated monthly for climate studies. Moreover, $XHWI_{N\,sum}$ is the sum of the index value for a day and H_{NZ} is the total number of hours during a day that the $XHWI_N$ index value was different from zero, that is:

$$XHWI_{N\,sum} = \sum\nolimits_{i=1}^{24} XHWI_{Ni} \qquad (16)$$

$$H_{NZ} = \sum\nolimits_{i=1}^{24} f_i \qquad (17)$$

in which $f_i = 1$ for hours where $XHWI_i > 0$ and 0 otherwise.

In order to illustrate the theoretical behavior of the $XHWI_N$, functions were used to show its exponential behavior and, especially, its dependence on relative humidity values (Figure 2). It is important to emphasize that relative humidity, as noted in many studies [43–45], plays a fundamental role in water loss from the bodies of different species, particularly during HW episodes.
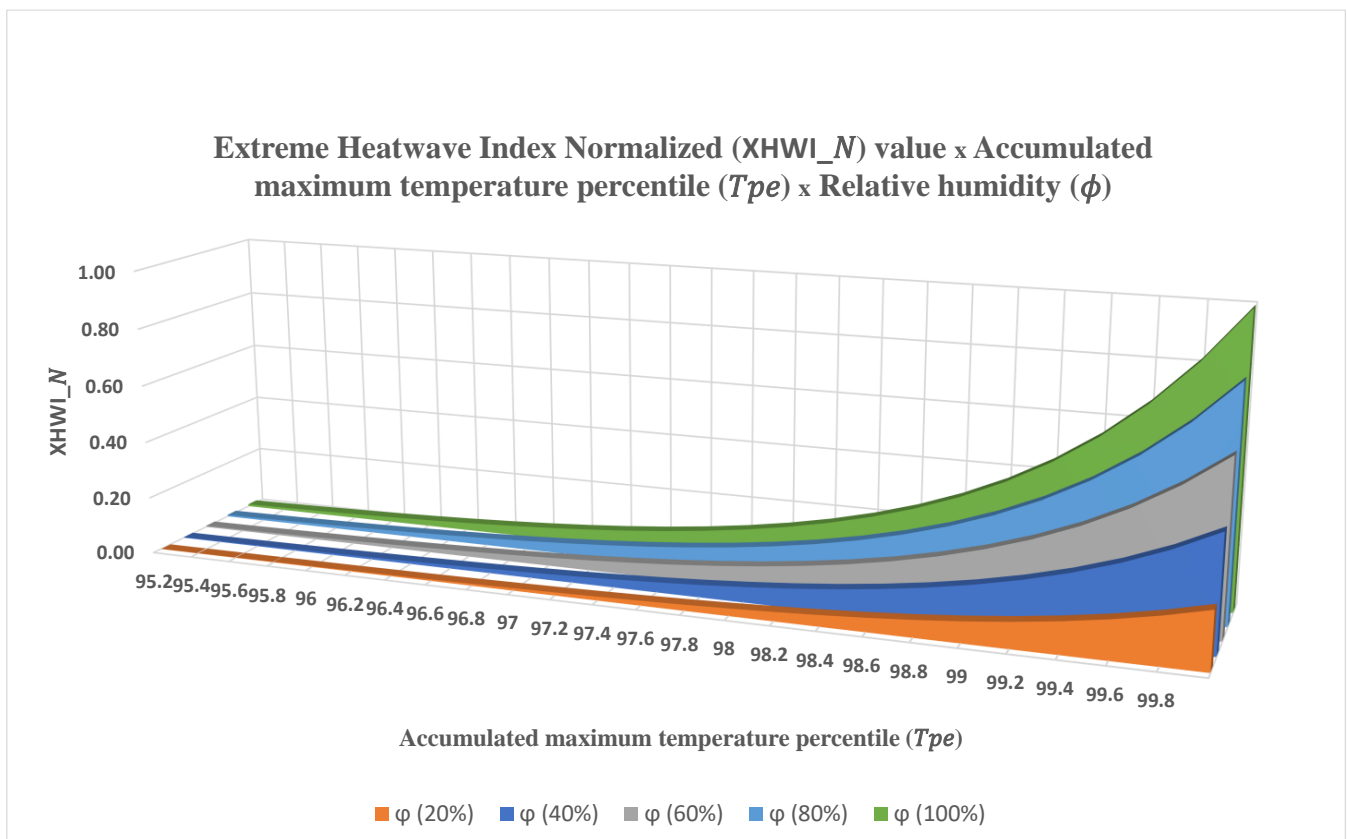

Figure 2. Theoretical behavior of the XHW Index.

As can be observed in Figure 2, the index value reaches 1 when the temperature values are at the 100th percentile of the cumulative distribution of maximum temperatures and the humidity is at 100%.

3.2. Application of the XHWI in the Detection of the Intensity and Duration of HW Episodes in the Summer of 2003 in Spain

This year was chosen because, according to numerous studies [46–49], the HW episode of 2003 was one of those that caused the highest number of deaths across the Iberian Peninsula.

To apply the index for detecting HW episodes, daily values ($XHWI_{N\,day}$) should be accumulated. This process starts by identifying the first day where the index value is greater than zero. From this day onward, each subsequent day's index value should be

added to that of the previous day, until a day when the index returns to zero is found. Upon finding this day, the accumulation is interrupted, and the accumulated index value resets to zero, restarting the process.

By proceeding in this way, it is possible to detect the duration of the HW episode and evaluate its intensity. Since the index is generalizable and relies exclusively on data from each location where it was calibrated, the intensity of the HW can be compared based on the index values across different regions without requiring any weighting or adjustment.

In order to evaluate the performance of the index in XHW situations, it was compared with maximum temperature anomaly data, obtained from the same ERA5 data, for the same location and based on the same climatology period (1960–1990). Additionally, these data were compared with weekly mortality data, obtained from [50].

3.3. Application of the XHWI Under Weather Forecast Conditions

To evaluate the application of the XHWI under weather forecast conditions, the WRF model [51] was run with the domain illustrated in Figure 3, with a spatial resolution of 1 km for the metropolitan region of Rio de Janeiro (mesh 1), using the set of physical parameterizations shown in Table 1. The spatial resolution decay relationship between the grids was 9 km–3 km–1 km.
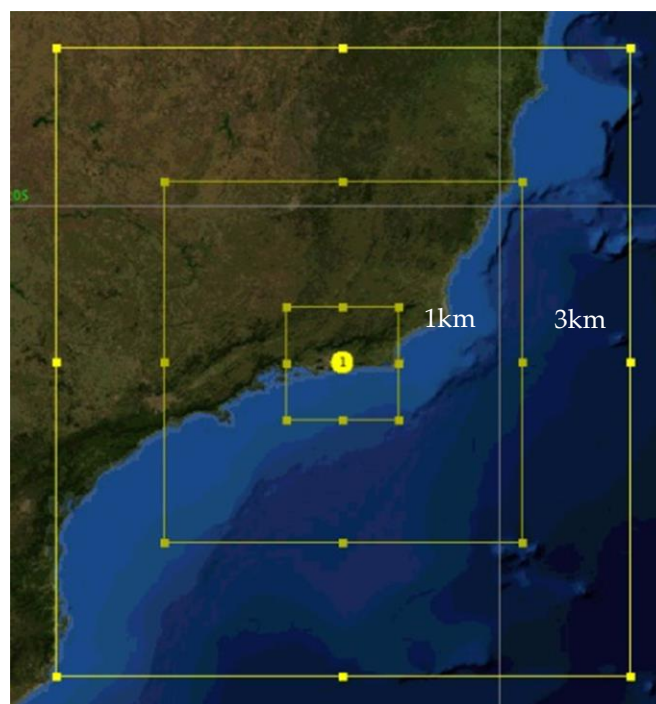

Figure 3. Domain and numerical grids used in the WRF simulations for the city of Rio de Janeiro. As the WRF is a regional model, it was nested using three grids, spatially arranged as illustrated in this figure. The outer yellow rectangle corresponds to the area of the grid with the lowest spatial resolution (9 km), the intermediate rectangle represents the medium-resolution grid (3 km), and the smallest rectangle indicates the area with the highest resolution (1 km), which was the grid used to calculate the HWI.

This phase was crucial for testing the application of the index under operational weather forecasting conditions and for assessing the complexity of seamless future integration of the index calculation directly into the model's code. This integration can be particularly important for generating climate projections, as the index requires hourly data for its calculation.

Table 1. Configuration of the parametric schemes used in the WRF Model simulations.

Physics	Option
Cloud Microphysics	WRF Single moment 3-class (3)
Shortwave and Longwave Radiation	Dudhia Shortwave (1) e RRTM Longwave scheme (1)
Surface Layer	Revised MM5 Scheme (2)
Land Surface	Unified Loah Land Surface Model (1)
Planetary Boundary Layer	Yonsei University Scheme (YSU) (1)
Cumulus and Convection	Kain-Fritsch Scheme (1)

The model was initialized with CFS analyses from 15 March 2024, at 00Z, simulating 5 days, until 19 March, 00Z, using GFS 0.25° forecasts every 6 h as lateral boundary conditions. This period was chosen for these simulations because between 17 and 19 March 2024, the metropolitan region of Rio de Janeiro recorded its highest historical air temperature values [52]. The XHW index (calibration and WRF simulation) was calculated for the coordinates −22.95 S and −41.3 W.

3.4. Use of the XHWI for Climate Studies

In order to evaluate the application of the index for climate studies, the index was calibrated for five cities in Spain (Figure 4), during the period of 1960 to 1990, using ERA5 data. For this work, the calibration considered all days in June, July, and August to compose the distribution of accumulated maximum temperatures.
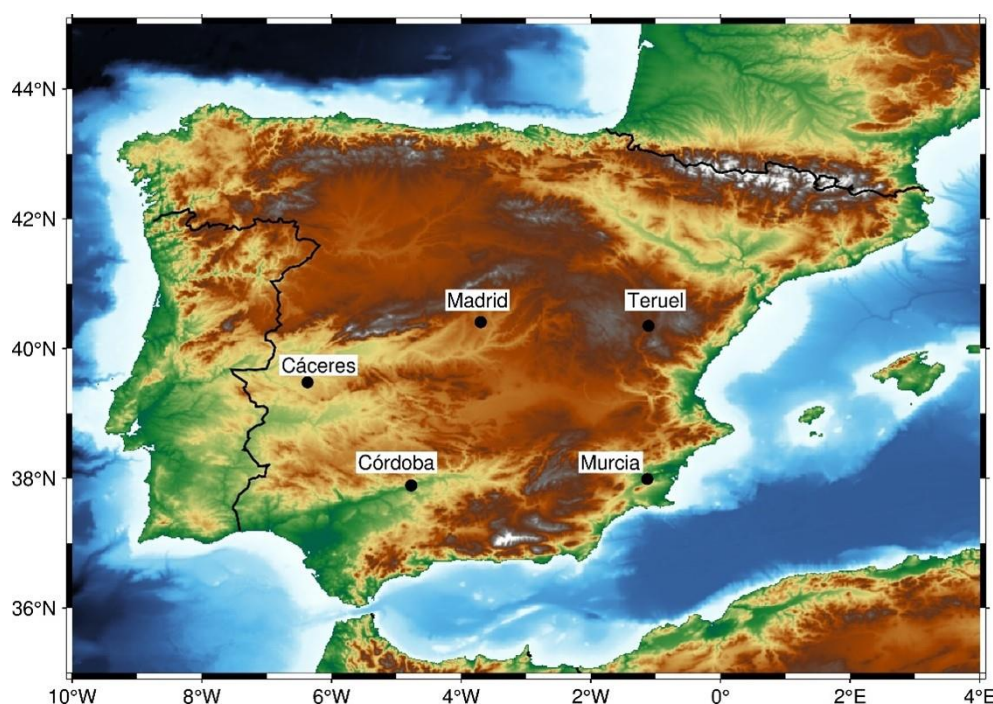
Figure 4. Map illustrating the geographical position of the five cities in Spain chosen for this study.

After calibration, hourly index normalized values $XHWI_{Ni}$ and daily accumulated values $XHWI_{Nsum}$ were calculated for June, July, and August from 1950 to 2022. Subsequently, the daily products of the index $XHWI_{Nday}$ were calculated based on Equation (15), then used to compose the monthly index value, which was simply the sum of the daily products values $XHWI_{Nday}$ for all days in the month. Finally, the annual index value was calculated as the sum of the index values for these three months. These values were accumulated in an area chart to assess possible trends in the index values over the analyzed period. Finally,

the results obtained with the HW index were compared, using the same analyses, with the data of the maximum temperature variation during the summer in the same cities.

4. Results

4.1. Assessment of the Index During the Summer of 2003 in Spain

Figure 5 displays the application of the accumulation $\text{XHWI}_{N\text{day}}$ for detecting XHW episodes in the five analyzed Spanish cities during the summer of 2003. In these figures, one can observe, in addition to the index values accumulated sequentially on days when the value remained above zero, the values of the maximum temperature anomaly and the weekly mortality anomalies, which were based on all the weeks of the summer of the same year.
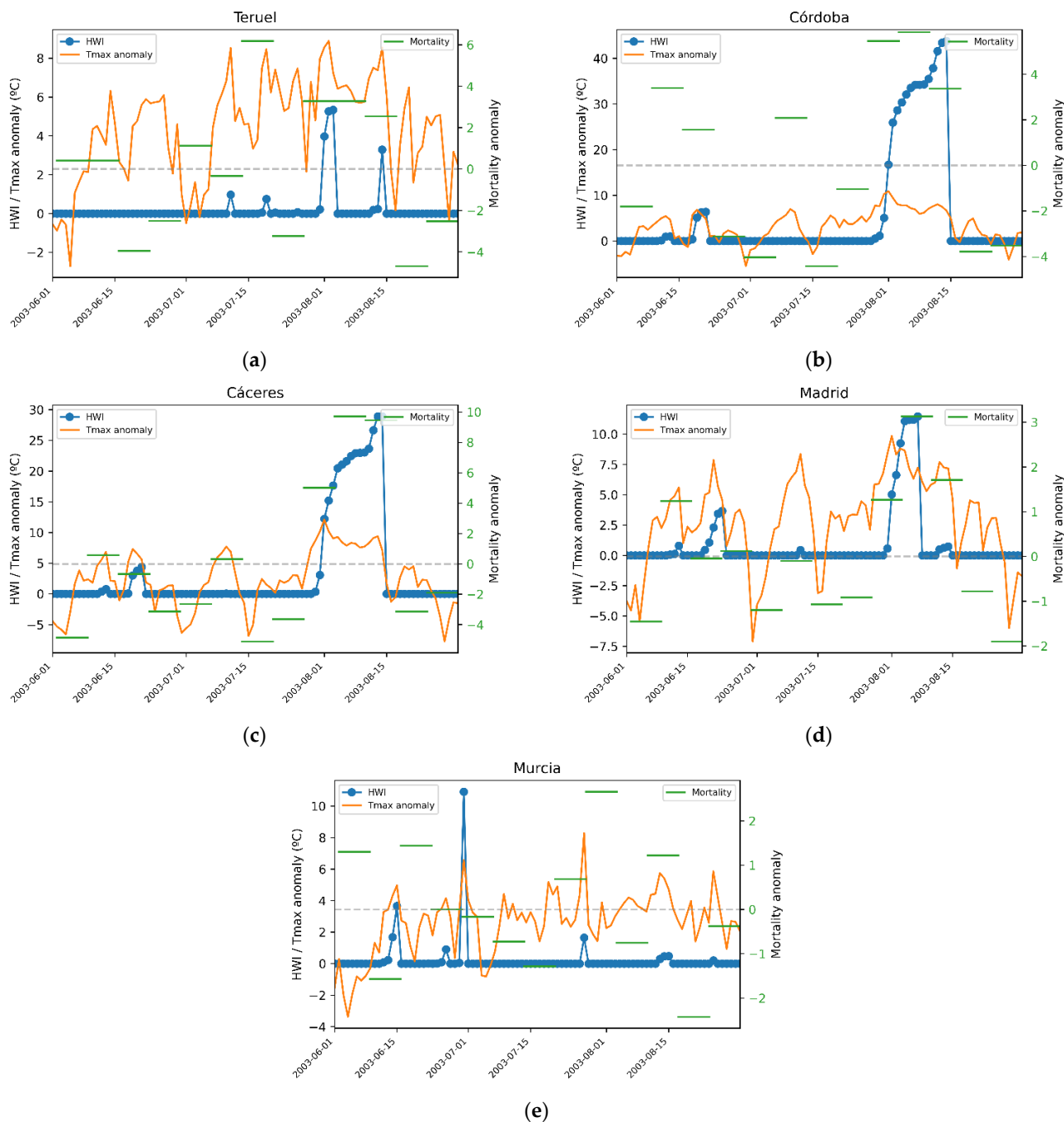

Figure 5. -Example of applying the XHWI for detecting HW episodes during the summer of 2003 in the cities of Teruel (**a**), Córdoba (**b**), Cáceres (**c**), Madrid (**d**), and Murcia (**e**).

If one considers three days as the minimum duration for detecting an HW episode, which aligns with the criteria defined, for instance, by Climate Adapt (European Environment Agency, n.d.), one can observe the occurrence of two XHW episodes in the cities of Teruel (5a), Córdoba (5b), Cáceres (5c), and Murcia (5e) and three in the city of Madrid (5d). The intensity and duration of the HW episodes varied significantly across the five cities. In most of them, the most intense HW was concentrated within the first 15 days of August, which also coincided with the highest mortality rates during this period.

In some cities, it became evident that there was a relationship between maximum temperature anomalies and mortality rates. However, it is important to highlight that in the cities of Córdoba, Cáceres, and Madrid, the weeks with the highest observed mortality rates were those where the index values were markedly higher, demonstrating the index's ability to detect critical HW periods associated with increased mortality.

In the cities of Teruel and Murcia, mortality rates did not respond to either temperature anomalies or the XHWI values. This can be easily understood for Murcia, as it did not experience any intense or prolonged HW episodes like the other cities. In Teruel, the two most intense HW episodes observed in August seemingly had some influence on the increased mortality during the two weeks in which they occurred. However, the highest mortality peak of the year was observed in middle of July, during a week situated between two periods where peaks in maximum temperature anomalies were observed, along with XHWI values a bit above zero (though only for one day). In the possible HW observed in July 2003, as well as in June of the same year in the city of Teruel, the recorded temperatures ranged between 29 and 31.9 °C. These temperatures did not fall within the range where the impact of rising temperatures on body water loss increases exponentially. In such cases, the relationship between temperature, relative humidity, and mortality rates can be assessed in a linear fashion, without the need for the index proposed in this study.

These results suggest that in 2003, particularly at the beginning of August, XHW events were responsible for the increase in mortality rates in 4 out of the 5 cities analyzed. This is much more evident when assessing the XHWI rather than solely evaluating maximum temperature anomalies, which means the index could be a crucial piece of data, especially for forecasting HWs and assessing health risks.

4.2. Application of the XHWI Weather Forecast Conditions

The following data present temperature forecast results obtained from the WRF simulations for 3 PM on 15 to 18 March 2024, in the metropolitan region of Rio de Janeiro, as shown in Figure 6. Special attention should be given to 17 March, which recorded the highest temperatures.

The hourly value of the index was calculated for the coordinates (-22.95 S; -41.3 W), as indicated in Figure 6c; subsequently, its daily $XHWI_{N\,day}$ (product of the hourly value of the $XHWI_N$ by the sum of the hours during which the index was different from zero) was calculated according to Equation (15). In Figure 7, the maximum observed temperature value for each day of the analyzed period is shown, as well as the number of hours in the day for which the index was greater than zero and the total value of $XHWI_{N\,day}$ for each day.

When comparing 16 March with 17 March, for example, it is important to note that the maximum temperature value increased by only about 8%, while the $XHWI_{N\,day}$ value increased by about 654%. This demonstrates the index's sensitivity to extreme temperature values, as well as the persistence of the HW episode, since there were 8 h with the index above zero on 17 March compared to only 4 h on 16 March.
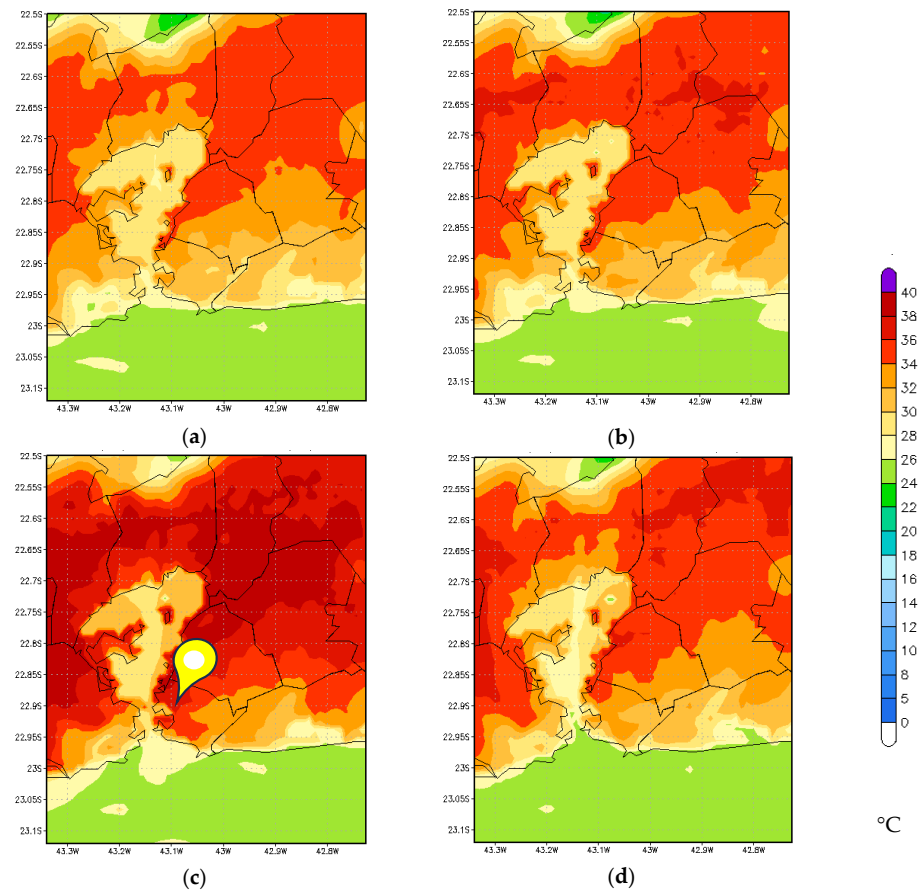
Figure 6. Results of the WRF simulations for air temperature at 2 m in degrees Celsius at 3 PM (maximum diary value) on 15 March (**a**), 16 (**b**), 17 (**c**), and 18 (**d**), 2024, for the Metropolitan Region of Rio de Janeiro, Brazil. On the x-axis are the longitude values, and on the y-axis are the latitude values.

Figure 7. Simulated values by the WRF of maximum temperature, hours when the XHW index was greater than zero, and the value of $XHWI_{N\,day}$ for the period between 15 and 18 March 2024.

4.3. Use of the Index for Climate Studies

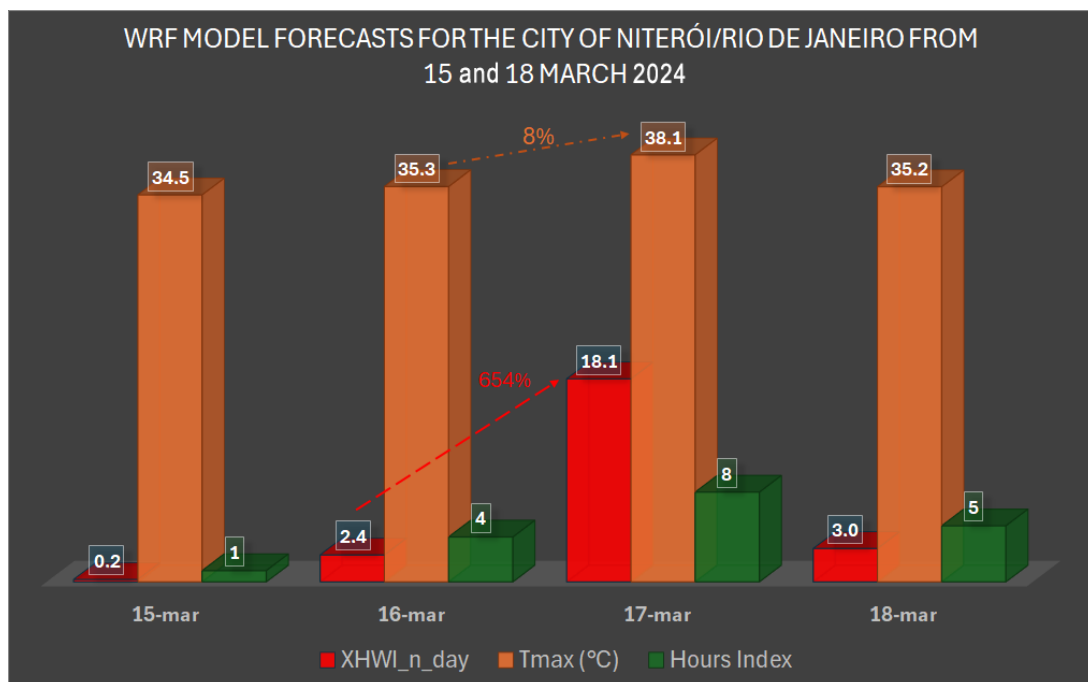As mentioned in Section 3.4, the XHWI value was accumulated annually for the cities of Murcia, Córdoba, Madrid, Teruel, and Cáceres in Spain to evaluate its annual behavior, specifically the accumulated values for June, July, and August, during the period from 1950 to 2022.

Figure 8 shows the accumulated area chart with the index calculated for all cities. By calculating the moving average over periods ranging between 20 and 30 years for the combined index of the five cities, three periods with the most distinct values were visually identified: the first period (P1) from 1950 to 1977; the second period (P2) from 1978 to 2002; and the third period (P3) from 2003 to 2022, as delineated in Figure 8.
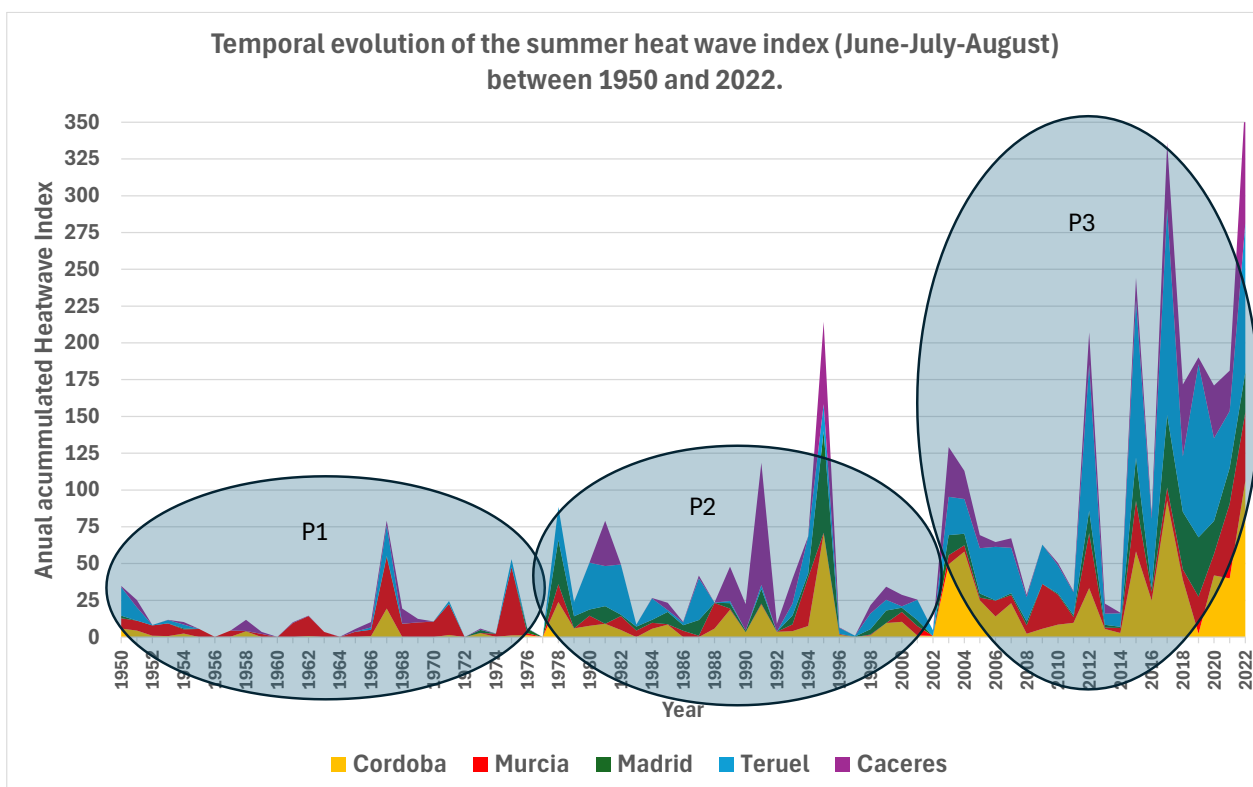

Figure 8. Temporal evolution of the accumulative summer XHWI (June-July-August) in the cities of Córdoba, Murcia, Madrid, Teruel, and Caceres between 1950 and 2022.

In order to compare the results obtained with the XHWI with respect to the increase in intensity and frequency of HWs in recent decades with a more traditional approach, the same analysis was replicated for the evolution of the maximum temperatures (obtained monthly average values) for the summers from 1950 to 2022, as portrayed in Figure 9. As can be seen, the use of maximum temperatures tends to smooth the evaluation of extreme events, as pointed out by some authors [53,54].

However, its use in this study served the didactic purpose of illustrating how the XHWI herein proposed is more suitable for evaluating extremes compared to simply analyzing the evolution of maximum temperature itself. In this way, the XHWI shows much greater sensitivity in identifying the increase in extreme episodes over time when compared to the analysis of the evolution of maximum temperature, as observed in the percentage differences in Tables 2 and 3, among the three time windows evaluated in this study.
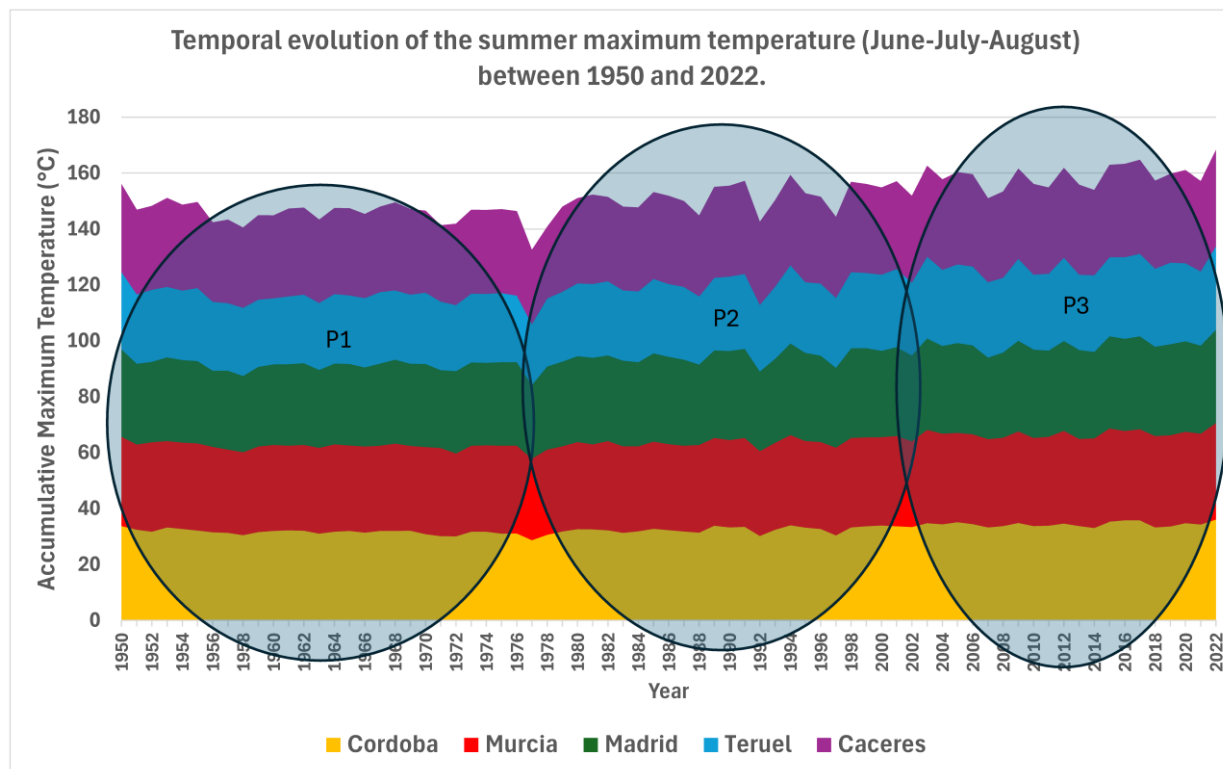
Figure 9. Temporal evolution of the accumulative summer maximum temperatures (June-July-August) in the cities of Córdoba, Murcia, Madrid, Teruel, and Caceres between 1950 and 2022.

Table 2. Average of summer accumulative XHWI values in the three periods (P1, P2, and P3).

City	1950–1977 (P1)	1978–2002 (P2)	2003–2022 (P3)	Percentage Increase P1 -> P2	Percentage Increase P2 -> P3	Percentage Increase P1 -> P3
Cordoba	1.9	7.5	31.8	301%	326%	1611%
Murcia	5.6	4.7	17.8	−17%	279%	217%
Madrid	0.9	8.4	20.3	820%	141%	2116%
Teruel	0.8	3.9	23.6	382%	508%	2831%
Carceres	1.9	9.9	18.5	419%	87%	872%
Average	*2.2*	*6.9*	*22.4*	*381%*	*268%*	*1529%*

Table 3. Average of summer maximum temperature values in the three periods (P1, P2, and P3).

City	1950–1977 °C (P1)	1978–2002 °C (P2)	2003–2022 °C (P3)	Percentage Increase P1 -> P2	Percentage Increase P2 -> P3	Percentage Increase P1 -> P3
Cordoba	31.6	32.5	34.5	3%	6%	9%
Murcia	30.7	31.2	32.4	1%	4%	5%
Madrid	29.0	30.8	31.9	6%	4%	10%
Teruel	24.6	26.0	28.1	6%	8%	14%
Carceres	30.1	30.9	32.3	3%	4%	7%
Average	*29.2*	*30.3*	*31.8*	*4%*	*5%*	*9%*

In other words, when we look at the average percentage increase in maximum temperatures between periods P1 and P3, for example, we see that this increase was 9%, which is indeed significant. However, when we examine this same increase in relation to the XHWI proposed in this study, we observe a rise of 1529%, as it accounts for the expo-

nential increase in extreme temperatures (above 32 °C and beyond the 95th percentile of maximum temperatures).

To quantitatively analyze whether the annual series of the XHWI and maximum temperatures exhibited a trend, the Mann–Kendall test was applied using the Python library "*pymannkendall*". The results are shown in Table 4. The analysis of the test parameters indicates that, for all cities, an upward trend was observed in both XHWI and maximum temperatures. Only in the city of Murcia did the p parameter value (0.002) for the XHWI trend approach the threshold where the positive trend would not be statistically significant, set at $p < 0.05$.

Table 4. Parameters obtained in the Mann–Kendall test for the annual series of the XHWI and maximum temperatures during the period from 1950 to 2022.

	Trend		P		Z		Tau	
	XHWI	**Max T**	**XHWI**	**Max T**	**XHWI**	**Max T**	**XHWI**	**Max T**
Murcia	increasing	increasing	0.002	6.16×10^{-10}	2.990	6.186	0.239	0.495
Caceres	increasing	increasing	1.61×10^{-6}	7.50×10^{-7}	4.797	4.948	0.384	0.396
Cordoba	increasing	increasing	4.82×10^{-10}	2.15×10^{-9}	6.225	5.986	0.498	0.479
Madrid	increasing	increasing	1.62×10^{-10}	3.30×10^{-13}	6.394	7.282	0.510	0.582
Teruel	increasing	increasing	4.00×10^{-10}	1.01×10^{-11}	6.254	6.805	0.495	0.544

Finally, based on the XHWI results, the probability of having at least one (Table 5), at least 10 (Table 6), and at least 15 (Table 7) days when the XHWI value was greater than zero (whether consecutive or not) during the summer was calculated for the three analyzed periods, illustrating how HWs have become much more frequent in period P3, as already shown in the studies by [55–57]. In this period, the probability of having at least one day with an XHW episode exceeds 80% in all cities, reaching 100% in Teruel and Córdoba. It is worth noting that, on average, this probability is three times higher in period P3 than in period P1, except in the city of Murcia, where the probability of having at least one day during the summer already exceeded 70% in period P1 and increased to 95% in period P3.

Table 5. Probability of experiencing at least one day with an XHWI value greater than zero during the summer across the five cities analyzed in this study.

City	1950–1977 (P1)	1978–2002 (P2)	2003–2022 (P3)
Córdoba	29%	84%	100%
Murcia	79%	52%	95%
Madrid	14%	84%	85%
Teruel	11%	56%	100%
Cáceres	39%	72%	90%

Table 6. Probability of experiencing at least 10 days with an XHWI value greater than zero during the summer across the five cities analyzed in this study.

City	1950–1977 (P1)	1978–2002 (P2)	2003–2022 (P3)
Córdoba	7%	60%	100%
Murcia	25%	16%	80%
Madrid	0%	60%	75%
Teruel	0%	4%	60%
Cáceres	18%	52%	80%

Table 7. Probability of experiencing at least 15 days with an XHWI value greater than zero during the summer across the five cities analyzed in this study.

City	1950–1977 (P1)	1978–2002 (P2)	2003–2022 (P3)
Córdoba	0%	24%	90%
Murcia	0%	0%	60%
Madrid	0%	16%	60%
Teruel	0%	0%	35%
Cáceres	4%	28%	60%

Regarding the probability of having at least 10 "XHW days" in the summer, that is, one HW day every six days, the probability increases in P3, reaching probabilities above 60% in all cities, with a notable highlight in Córdoba, where the probability hit 100% for years with more than 10 days of XHWI values greater than zero. Meanwhile, the probability of having at least 15 "XHW days" in the summer, that is, one HW day every four days, reaches a staggering 60% in Murcia, Madrid, and Cáceres and 90% in Córdoba.

In fact, the city of Córdoba averaged 30 days with XHWI values greater than zero during the P3 period, meaning that in this period, one out of every three summer days presented extreme heat conditions. These values were approximately 5 days in P1 (1 out of every 18 summer days) and 12 days in P2 (1 out of every 7.5 summer days).

5. Discussion

- **Conceptual evaluation of XHWI**

In terms of its theoretical profile, the XHWI was shown to fully align with the initial hypothesis, displaying a pronounced exponential increase in extreme temperature values alongside a clear dependence on relative humidity, as demonstrated in Figure 4, which illustrates its theoretical framework.

The approach utilized to calibrate the XHWI for detecting XHW events proved highly effective when applied to the 2003 HW episodes in Spain. The index exhibited remarkable sensitivity in identifying the most extreme episodes, specifically those associated with the highest anomalies in mortality rates. Although maximum temperature anomalies were found to correlate reasonably well with variations in mortality rates, they did not, at least in the analyses conducted in this study, demonstrate adequate sensitivity to anticipate potential periods of heightened health risks and, consequently, increased mortality. In contrast, the XHWI showed superior performance in this regard.

When evaluating the applicability of the index for climate analysis, the XHWI demonstrated substantially greater sensitivity in diagnosing the intensification and persistence of HWs over recent decades compared to maximum temperature values alone. This makes it a particularly valuable tool for the study of extreme climate events. Furthermore, the index proved to be a reliable instrument for identifying extreme events and can also serve as an educational tool to illustrate the concept of "more frequent and extreme events" in the context of climate change.

- **Results of XHWI and its applications in assessing risk prevention and alert emission**

The XHWI has demonstrated its utility in weather forecasting by enabling the issuance of HW alerts, including the quantification of both the intensity and duration of XHW episodes. However, further research is needed to cross-reference XHWI data with hospitalization and mortality records associated with HWs across different cities and countries. Such studies would allow for the creation of risk thresholds, improving communication and the effectiveness of alerts to the population.

When examining the temporal evolution of XHW episodes in the five Spanish cities studied, it becomes apparent that it is easier, visually, to identify the increasing number, intensity, and duration of XHW events over time through the graphical representation of the XHWI (Figure 8) rather than through the evolution of maximum temperatures (Figure 9).

Moreover, analyzing the annual variation of maximum temperatures does not clearly indicate the years with the greatest health risks linked to XHW events during the period from 1950 to 2022. In contrast, tracking the evolution of the accumulated annual XHWI values (2003, 2012, 2015, 2018, and 2022) allows for the identification of these high-risk years. These years have also been cited by other authors as reference periods for HW occurrences in Spain, based on alternative detection methodologies [48,56,58]. However, in this study, these years were identified solely based on the intensity and duration of the events using the XHWI.

In analyzing period P3, it is clear that XHW events began to occur more frequently and with greater intensity in most years of this period, compared to previous periods (P1 and P2), except for 2013 and 2014.

The rise in XHWI values in recent years highlights the increased potential risk faced by certain cities, particularly those that registered the highest index values during the most recent analyzed period (P3). Overall, all cities showed a significant increase in the intensity and duration of XHW episodes over the past few decades. On average, there was a 1529% increase in XHWI values during period P3 compared to period P1 (Table 2).

These findings are alarming and provide a clearer understanding of the escalating situation regarding HWs in Spain over recent decades [55–57]. Such a diagnosis would not have been possible by analyzing only the increase in maximum temperatures during this period, which rose by just 9% when comparing period P3 to period P1 (Table 3).

- **Further studies**

Despite the significance of the current findings, further studies are required to simulate the relationship between the XHWI and blood water loss rates. This research would provide essential insights for informing the population about appropriate water intake during HW episodes, specifying the necessary quantity (which may vary according to physiological factors) and the expected duration of the HW.

Finally, for a comprehensive understanding of the relationship between XHWI values and associated potential health risks, additional studies should be conducted, incorporating factors such as age, gender, pre-existing medical conditions, and the level of preparedness in different populations and cities. These factors played a critical role during past HW episodes, such as the one in 2003 [58–60]. It is worth noting that Météo-France has made efforts in this direction in recent years, as can be observed in [61], illustrating the importance of comprehensive risk assessments.

Upon completion of such studies, the XHWI could evolve into a robust, stable, and globally generalizable methodology for defining XHW episodes anywhere in the world. This potential lies in the fact that the proposed index is based on region-specific data and the historical record of extreme temperatures, rather than relying on a fixed temperature threshold. Consequently, it could serve as a standardized global metric for defining the intensity and duration of XHW episodes, something that currently does not exist [54,62].

The adoption of a standardized index for defining meteorological and climatic events, similar to indices developed by [63–65], is of critical importance and would enable a greater number of scientists to provide a framework that allows for a fair/fairer intercomparison with other works on extreme weather/climate phenomena [66].

6. Conclusions

This study represents the first step in the development of a new multivariate XHWI, designed to support a health impact-based forecasting system that includes a mitigation action plan with hydration-related measures. In the final version of the XHWI, it is expected that this new index will be more suitable/adapted for identifying the XHW episodes posing the greatest danger to human health.

This initial, more generalized version of the index, due to the premises used in its formulation, tends to exponentially emphasize extreme events, already demonstrating a strong performance in detecting and measuring the duration of XHW episodes. Moreover, the inclusion of relative humidity in the index improves its ability to account for factors

affecting human health, as relative humidity plays a crucial role in water loss for nearly all living organisms.

Future research should be focused on calibrating the index threshold values based on health risks associated with XHW episodes. These studies should, as much as possible, integrate simulations of body water loss processes and their relationship to cardiovascular events such as heart attacks. Through this calibration, thresholds can be established to define various risk levels for populations across the index's value range (0 to 1), allowing the index to be adapted in different regions without requiring mathematical alterations.

Following this final stage, the index should be evaluated against other existing indices that incorporate at least one of the physical principles used in the development of the XHWI. This comparison should utilize mortality data from the widest possible range of locations and XHW events, ensuring a comprehensive analysis.

Finally, the authors think that the XHWI could serve as a valuable tool for identifying extreme mortality events related to XHW occurrences in climate change projections, not only in Europe but globally. The index's design allows it to be applied in regions lacking extensive atmospheric measurement networks, while also incorporating the physical mechanisms linked to major health risks posed by XHWs. Its universality and ability to be replicated anywhere on the planet provide an essential insight for better understanding and preparing for the future of XHW events.

Author Contributions: Conceptualization, M.C.; Methodology, L.A.S. and G.G.-M.; Software, V.L.V.G.; Formal analysis, V.G.; Data curation, L.M.P.; Supervision, J.P.M. and P.J.-G. All authors have read and agreed to the published version of the manuscript.

Institutional Review Board Statement: Not applicable.

Informed Consent Statement: Not applicable.

Data Availability Statement: The data presented in this study are available on request from the corresponding author. The data are not publicly available due to privacy.

Conflicts of Interest: The authors declare no conflicts of interest.

References

1. Campbell, S.; Remenyi, T.A.; White, C.J.; Johnston, F.H. Heatwave and health impact research: A global review. *Health Place* **2018**, *53*, 210–218. [CrossRef] [PubMed]
2. Kamel Boulos, M.N.; Wilson, J.P. Geospatial techniques for monitoring and mitigating climate change and its effects on human health. *Int. J. Health Geogr.* **2023**, *22*, 2. [CrossRef]
3. Bi, X.; Wu, C.; Wang, C.; Wang, Y.; Wang, X.; Song, C.; Li, J.; Fu, C. Impacts of air temperature and its extremes on human mortality in Shanghai, China. *Urban Clim.* **2022**, *41*, 101072. [CrossRef]
4. Lu, R.; Xu, K.; Chen, R.; Chen, W.; Li, F.; Lv, C. Heat waves in summer 2022 and increasing concern regarding heat waves in general. *Atmos. Ocean. Sci. Lett.* **2023**, *16*, 100290. [CrossRef]
5. Moraes, S.L.; Almendra, R.; Barrozo, L.V. Impact of heat waves and cold spells on cause-specific mortality in the city of São Paulo, Brazil. *Int. J. Hyg. Environ. Health* **2022**, *239*, 113861. [CrossRef]
6. Błażejczyk, K.; Twardosz, R.; Wałach, P.; Czarnecka, K.; Błażejczyk, A. Heat strain and mortality effects of prolonged central European heat wave-an example of June 2019 in Poland. *Int. J. Biometeorol.* **2022**, *66*, 149–161. [CrossRef]
7. Winklmayr, C.; Muthers, S.; Niemann, H.; Mücke, H.G.; an der Heiden, M. Heat-related mortality in Germany from 1992 to 2021. *Dtsch. Arztebl. Int.* **2022**, *119*, 451–457. [CrossRef]

8. Wedler, M.; Pinto, J.G.; Hochman, A. More frequent, persistent, and deadly heat waves in the 21st century over the Eastern Mediterranean. *Sci. Total Environ.* **2023**, *870*, 161883. [CrossRef]

9. Foroni, M.; Salvioli, G.; Rielli, R.; Goldoni, C.A.; Orlandi, G.; Sajani, S.Z.; Guerzoni, A.; Maccaferri, C.; Daya, G.; Mussi, C. A Retrospective Study on Heat-Related Mortality in an Elderly Population During the 2003 Heat Wave in Modena, Italy: The Argento Project. *J. Gerontol. Ser. A* **2007**, *62*, 647–651. [CrossRef] [PubMed]

10. Palinkas, L.A.; Hurlburt, M.S.; Fernandez, C.; De Leon, J.; Yu, K.; Salinas, E.; Garcia, E.; Johnston, J.; Rahman, M.M.; Silva, S.J.; et al. Vulnerable, Resilient, or Both? A Qualitative Study of Adaptation Resources and Behaviors to Heat Waves and Health Outcomes of Low-Income Residents of Urban Heat Islands. *Int. J. Environ. Res. Public Health* **2022**, *19*, 11090. [CrossRef]

11. Ebi, K.L.; Vanos, J.; Baldwin, J.W.; Bell, J.E.; Hondula, D.M.; Errett, N.A.; Hayes, K.; Reid, C.E.; Saha, S.; Spector, J.; et al. Extreme Weather and Climate Change: Population Health and Health System Implications. *Annu. Rev. Public Health* **2021**, *42*, 293–315. [CrossRef]

12. Wang, Z.; Hong, T.; Li, H. Informing the planning of rotating power outages in heat waves through data analytics of connected smart thermostats for residential buildings. *Environ. Res. Lett.* **2021**, *16*, 74003. [CrossRef]

13. Zhao, L.; Oleson, K.; Bou-Zeid, E.; Krayenhoff, E.S.; Bray, A.; Zhu, Q.; Zheng, Z.; Chen, C. Global multi-model projections of local urban climates. *Nat. Clim. Chang.* **2021**, *11*, 152–157. [CrossRef]

14. Rahman, M.M.; McConnell, R.; Schlaerth, H.; Ko, J.; Silva, S.; Lurmann, F.W.; Palinkas, L.; Johnston, J.; Hurlburt, M.; Yin, H.; et al. The effects of coexposure to extremes of heat and particulate air pollution on mortality in California: Implications for climate change. *Am. J. Respir. Crit. Care Med.* **2022**, *206*, 1117–1127. [CrossRef]

15. Xu, R.; Huang, S.; Shi, C.; Wang, R.; Liu, T.; Li, Y.; Zheng, Y.; Lv, Z.; Wei, J.; Sun, H.; et al. Extreme Temperature Events, Fine Particulate Matter, and Myocardial Infarction Mortality. *Circulation* **2023**, *148*, 312–323. [CrossRef] [PubMed]

16. Smoyer-Tomic, K.E.; Kuhn, R.; Hudson, A. Heat Wave Hazards: An Overview of Heat Wave Impacts in Canada. *Nat. Hazards* **2003**, *28*, 465–486. [CrossRef]

17. Robine, J.-M.; Cheung, S.L.K.; Le Roy, S.; Van Oyen, H.; Griffiths, C.; Michel, J.P.; Herrmann, F.R. Death toll exceeded 70,000 in Europe during the summer of 2003. *Comptes. Rendus. Biol.* **2008**, *331*, 171–178. [CrossRef] [PubMed]

18. Hoag, H. Russian summer tops 'universal' heatwave index. *Nature* **2014**, *16*, 636. [CrossRef]

19. Li, M.; Gu, S.; Bi, P.; Yang, J.; Liu, Q. Heat Waves and Morbidity: Current Knowledge and Further Direction-A Comprehensive Literature Review. *Int. J. Environ. Res. Public Health* **2015**, *12*, 5256–5283. [CrossRef] [PubMed]

20. Mazdiyasni, O.; AghaKouchak, A.; Davis, S.J.; Madadgar, S.; Mehran, A.; Ragno, E.; Sadegh, M.; Sengupta, A.; Ghosh, S.; Dhanya, C.T.; et al. Increasing probability of mortality during Indian heat waves. *Sci. Adv.* **2017**, *3*, e1700066. [CrossRef]

21. Meehl, G.A.; Tebaldi, C. More intense, more frequent, and longer lasting heat waves in the 21st century. *Science* **2004**, *305*, 994–997. [CrossRef] [PubMed]

22. IPCC. *2021: Climate Change 2021: The Physical Science Basis. Contribution of Working Group I to the Sixth Assessment Report of the Intergovernmental Panel on Climate Change*; Masson-Delmotte, V., Zhai, P., Pirani, A., Connors, S.L., Péan, C., Berger, S., Caud, N., Chen, Y., Goldfarb, L., Gomis, M.I., et al., Eds.; Cambridge University Press: Cambridge, UK, 2021.

23. Our World in Data. (n.d.). Our World in Data. Available online: https://ourworldindata.org/ (accessed on 8 March 2024).

24. Casanueva, A.; Burgstall, A.; Kotlarski, S.; Messeri, A.; Morabito, M.; Flouris, A.D.; Nybo, L.; Spirig, C.; Schwierz, C. Overview of Existing Heat-Health Warning Systems in Europe. *Int. J. Environ. Res. Public Health* **2019**, *16*, 2657. [CrossRef]

25. Keatinge, W.R. Death in heat waves. *BMJ* **2003**, *327*, 512–513. [CrossRef] [PubMed]

26. Keatinge, W.R.; Coleshaw, S.R.K.; Easton, J.C.; Cotter, F.; Mattock, M.B.; Chelliah, R. Increased platelet and red cell counts, blood viscosity, and plasma cholesterol levels during heat stress, and mortality from coronary and cerebral thrombosis. *Am. J. Med.* **1986**, *81*, 795–800. [CrossRef]

27. Mora, C.; Dousset, B.; Caldwell, I.R.; Powell, F.E.; Geronimo, R.C.; Bielecki, C.R.; Counsell, C.W.; Dietrich, B.S.; Johnston, E.T.; Louis, L.V.; et al. Global risk of deadly heat. *Nat. Clim. Chang.* **2017**, *7*, 501–506. [CrossRef]

28. Muthers, S.; Laschewski, G.; Matzarakis, A. The Summers 2003 and 2015 in South-West Germany: Heat Waves and Heat-Related Mortality in the Context of Climate Change. *Atmosphere* **2017**, *8*, 224. [CrossRef]

29. Schaeffer, L.; de Crouy-Chanel, P.; Wagner, V.; Desplat, J.; Pascal, M. How to estimate exposure when studying the temperature-mortality relationship? A case study of the Paris area. *Int. J. Biometeorol.* **2016**, *60*, 73–83. [CrossRef]

30. Mitchell, D.; Heaviside, C.; Vardoulakis, S.; Huntingford, C.; Masato, G.; Guillod, B.P.; Frumhoff, P.; Bowery, A.; Wallom, D.; Allen, M. Attributing human mortality during extreme heat waves to anthropogenic climate change. *Environ. Res. Lett.* **2016**, *11*, 7. [CrossRef]

31. Mora, C.; Counsell, C.W.W.; Bielecki, C.R.; Louis, L.V. Twenty-Seven Ways a Heat Wave Can Kill You: Deadly Heat in the Era of Climate Change. *Cardiovasc. Qual. Outcomes* **2017**, *10*, e004233. [CrossRef]

32. Wenger, C.B. Human heat acclimatization. In *Human Performance Physiology and Environmental Medicine at Terrestrial Extremes*; Benchmark Press: Concord, NC, USA, 1988; pp. 153–197.

33. Wyndham, C.H.; Atkins, A.R. A Physiological Scheme and Mathematical Model of Temperature Regulation in Man. *Pflügers Arch. Eur. J. Physiol.* **1968**, *303*, 14–30. [CrossRef] [PubMed]

34. Cengel, Y.A.; Ghajar, A. *Heat and Mass Transfer: Fundamentals and Applications*, 6th ed.; McGraw Hill: New York, NY, USA, 2021.

35. Sphaier, L.A.; Worek, W.M. Analysis of heat and mass transfer in porous sorbents used in rotary regenerators. *Int. J. Heat Mass Transf.* **2004**, *47*, 3415–3430. [CrossRef]

36. ASHRAE. *ASHRAE Handbook Fundamentals*; American Society of Heating, Refrigerating and Air-conditioning Engineers: Atlanta, GA, USA, 2005.

37. Nadel, E.R.; Stolwijk, J.A. Effect of exposure to hot environments on the level of dehydration in resting and exercising men. *J. Appl. Physiol.* **1973**, *35*, 698–704.

38. Sawka, M.N.; Montain, S.J. Fluid and electrolyte supplementation for exercise heat stress. *Am. J. Clin. Nutr.* **2000**, *72*, 564S–572S. [CrossRef] [PubMed]

39. Kenny, G.P.; Jay, O. Thermometry, calorimetry, and mean body temperature during heat stress. *Compr. Physiol.* **2013**, *3*, 1689–1719. [CrossRef] [PubMed]

40. Hersbach, H.; Bell, B.; Berrisford, P.; Hirahara, S.; Horányi, A.; Muñoz-Sabater, J.; Nicolas, J.; Peubey, C.; Radu, R.; Schepers, D.; et al. The ERA5 global reanalysis. *Q. J. R. Meteorol. Soc.* **2020**, *146*, 1999–2049. [CrossRef]

41. Awasthi, A.; Vishwakarma, K.; Pattnayak, K.C. Retrospection of heatwave and heat index. *Theor. Appl. Clim.* **2022**, *147*, 589–604. [CrossRef]

42. Weather Underground. (n.d.). World Record for Low Humidity: 116 °F with 0.36% Humidity in Iran. Available online: https://www.wunderground.com/cat6/world-record-low-humidity-116f-036-humidity-iran- (accessed on 21 February 2024).

43. Chen, X.; Li, N.; Liu, J.; Zhang, Z.; Liu, Y. Global Heat Wave Hazard Considering Humidity Effects during the 21st Century. *Int. J. Environ. Res. Public Health* **2019**, *16*, 1513. [CrossRef]

44. Rastogi, D.; Lehner, F.; Ashfaq, M. Revisiting recent U.S. heat waves in a warmer and more humid climate. *Geophys. Res. Lett.* **2020**, *47*, e2019GL086736. [CrossRef]

45. Russo, S.; Sillmann, J.; Sterl, A. Humid heat waves at different warming levels. *Sci. Rep.* **2017**, *7*, 7477. [CrossRef] [PubMed]

46. Díaz-Poso, A.; Lorenzo, N.; Royé, D. Spatio-temporal evolution of heat waves severity and expansion across the Iberian Peninsula and Balearic islands. *Environ. Res.* **2023**, *217*, 114864. [CrossRef]

47. Tobías, A.; Royé, D.; Iñiguez, C. Heat-attributable Mortality in the Summer of 2022 in Spain. *Epidemiology* **2023**, *34*, e5–e6. [CrossRef]

48. Serrano-Notivoli, R.; Tejedor, E.; Sarricolea, P.; Meseguer-Ruiz, O.; de Luis, M.; Saz, M.Á.; Longares, L.A.; Olcina, J. Unprecedented warmth: A look at Spain's exceptional summer of 2022. *Atmos. Res.* **2023**, *293*, 106931. [CrossRef]

49. Tripathy, K.P.; Mishra, A.K. How unusual is the 2022 European compound drought and heatwave event? *Geophys. Res. Lett.* **2023**, *50*, e2023GL105453. [CrossRef]

50. European Statistical Office (Eurostat). 2024. Database. Available online: https://ec.europa.eu/eurostat/web/main/data/database (accessed on 30 May 2024).

51. Skamarock, W.C.; Klemp, J.B.; Dudhia, J.; Gill, D.O.; Liu, Z.; Berner, J.; Wang, W.; Powers, J.G.; Duda, M.G.; Barker, D.M.; et al. *2019: A Description of the Advanced Research WRF Version 4*; NCAR Tech. Note NCAR/TN-556+STR; 2019; 145p. [CrossRef]

52. Down To Earth. (n.d.). Climate Crisis Everywhere All at Once: Record-Breaking Temperature in 10 Countries Across 4 Continents. Available online: https://www.downtoearth.org.in/news/climate-change/climate-crisis-everywhere-all-at-once-record-breaking-temperature-in-10-countries-across-4-continents-95110 (accessed on 10 June 2024).

53. Perkins, S.E.; Alexander, L.V. On the Measurement of Heat Waves. *J. Clim.* **2013**, *26*, 4500–4517. [CrossRef]

54. Heo, S.; Bell, M.L.; Lee, J.-T. Comparison of health risks by heat wave definition: Applicability of wet-bulb globe temperature for heat wave criteria. *Environ. Res.* **2019**, *168*, 158–170. [CrossRef] [PubMed]

55. Royé, D.; Codesido, R.; Tobías, A.; Taracido, M. Heat wave intensity and daily mortality in four of the largest cities of Spain. *Environ. Res.* **2020**, *182*, 109027. [CrossRef]

56. Paredes-Fortuny, L.; Khodayar, S. Understanding the Magnification of Heatwaves over Spain: Relevant changes in the most extreme events. *Weather Clim. Extrem.* **2023**, *42*, 100631. [CrossRef]

57. López-Bueno, J.A.; Díaz, J.; Follos, F.; Vellón, J.M.; Navas, M.A.; Culqui, D.; Luna, M.Y.; Sánchez-Martínez, G. Evolution of the threshold temperature definition of a heat wave vs. evolution of the minimum mortality temperature: A case study in Spain during the 1983–2018 period. *Environ. Sci. Eur.* **2021**, *33*, 101. [CrossRef]

58. Díaz, J.; García-Herrera, R.; Trigo, R.M.; Linares, C.; Valente, M.A.; De Miguel, J.M.; Hernández, E. The impact of the summer 2003 heat wave in Iberia: How should we measure it? *Int. J. Biometeorol.* **2006**, *50*, 159–166. [CrossRef]

59. García-Herrera, R.; Díaz, J.; Trigo, R.M.; Luterbacher, J.; Fischer, E.M. A Review of the European Summer Heat Wave of 2003. *Crit. Rev. Environ. Sci. Technol.* **2010**, *40*, 267–306. [CrossRef]

60. Fouillet, A.; Rey, G.; Laurent, F.; Pavillon, G.; Bellec, S.; Guihenneuc-Jouyaux, C.; Clavel, J.; Jougla, E. Excess mortality related to the August 2003 heat wave in France. *Int. Arch. Occup. Environ. Health* **2006**, *80*, 16–24. [CrossRef]

61. Santé Publique France. (2022, December 20). Bulletin de Santé Publique—Heatwaves, France—Summer 2022. Santé Publique France. Available online: https://www.santepubliquefrance.fr/en/bulletin-de-sante-publique-heatwaves-france-summer-2022 (accessed on 12 June 2024).

62. Guo, Y.; Gasparrini, A.; Armstrong, B.G.; Tawatsupa, B.; Tobias, A.; Lavigne, E.; de Sousa Zanotti Stagliorio Coelho, M.; Pan, X.; Kim, H.; Hashizume, M.; et al. Heat Wave and Mortality: A Multicountry, Multicommunity Study. *Environ. Health Perspect.* **2017**, *125*, 87006. [CrossRef] [PubMed]

63. Nielsen, D.M.; Belém, A.L.; Marton Cataldi, M. Dynamics-based regression models for the South Atlantic Convergence Zone. *Clim. Dyn.* **2019**, *52*, 5527–5553. [CrossRef]

64. Cataldi, M.; Ribeiro, E.M.; Andrade, L.S.; Pandolfi de Lima, A.; Almeida, G.L.M.; Pereira, T.R.A. Creation and Assessment of an Index for Atmospheric Blockings in Brazil's Central Region. *Adv. Hydro Meteorol.* **2024**, *1*. [CrossRef]
65. Da Silveira, L.H.M.; Cataldi, M.; de Farias, W.C.M. Development of multi-scale indices of human mobility restriction during the COVID-19 based on air quality from local and global NO_2 concentration. *ISCIENCE* **2023**, *26*, 107599. [CrossRef] [PubMed]
66. Da Fonseca Aguiar, L.; Cataldi, M. Social and environmental vulnerability in Southeast Brazil associated with the South Atlantic Convergence Zone. *Nat. Hazards* **2021**, *109*, 2423–2437. [CrossRef]